Raman Spectroscopic Study of the Solvation of Decafluorobenzophenone Ketyl Radical and Related Compounds in 2-Propanol at Ambient to Supercritical Temperatures

Tomotsumi Fujisawa,[†] Takanori Ito,[†] Masahide Terazima,[†] and Yoshifumi Kimura*[,‡]

Department of Chemistry, Graduate School of Science, Kyoto University, Kyoto, 606-8502, Japan, and Division of Research Initiative, International Innovation Center, Kyoto University, Kyoto, 606-8501, Japan

Received: September 10, 2007; In Final Form: December 5, 2007

Time-resolved Raman spectroscopy has been applied to the hydrogen-abstraction reaction of decafluorobenzophenone (DFBP) from 2-propanol in temperatures ranging from room to supercritical temperature (520 K) at 31 MPa. The Raman bands of the intermediate ketyl radical (DFBPK) were identified. The Raman bands assigned to the C═C stretching mode (1639 cm^{-1}) and the C−O stretching modes (1274 cm^{-1}) shift to lower frequencies with increasing temperature. The corresponding Raman bands of stable molecules (reference molecules), benzhydrol, decafluorobenzhydrol, and benzophenone (BP), which all have similar molecular structures to those of DFBP or DFBPK, were also investigated at the same range of temperatures. Assignments of the Raman bands were performed with the help of density functional theoretical calculations and the isotopic exchange method. By comparing the Raman peak shifts of the radical with those of the reference molecules, the shift of the C═C stretching mode with increasing temperature (or decrease in the solvent density) is considered to be primarily due to the decrease in the repulsive interaction between the solute and the solvent. On the other hand, the shift of the C−O stretching mode of the radical reflects the decrease in the solvent Lewis acidity or its hydrogen-bonding donating ability, which is clearly illustrated by the shifts of the C═O stretching mode of BP and the C−O stretching mode of 2-propanol. The frequency of the C−O stretching mode of DFBPK was relatively sensitive to the surrounding environment. It was observed that the bandwidth of the radical was generally large, and this observation supports the previous report by Terazima and Hamaguchi (Terazima, M.; Hamaguchi, H. *J. Chem. Phys.* **1995**, *99*, 7891). Additionally, the sensitivity and the deformability of the radical structure due to the change of the solvent temperature and density were revealed in our studies.

1. Introduction

Supercritical fluids with hydrogen-bonding ability such as supercritical water (SCW) and supercritical alcohols are a new class of solvent fluids that enable us to develop new types of chemical reactions and have been attracting attention from chemists in academia and industry alike.[1−4] In particular, the structure and dynamics related to the hydrogen bonding of SCW and supercritical methanol (SCMe) have been studied by various spectroscopic methods, such as neutron and X-ray scattering, NMR, Raman scattering, and so forth.[5−12] These studies have revealed answers to many questions, including the question of how the hydrogen bonding exists in such fluids near the critical point and how it affects the molecular dynamics of solvent molecules.

However, spectroscopic studies on the solvation in SCW and supercritical alcohols are still limited. To understand chemical reactions occurring in these fluids, the knowledge of the solvation of a short-lived reaction intermediate as well as a stable molecule is crucial. However, most studies focus on the measurements of solvatochromic shifts and fluorescence Stokes shifts of stable solvatochromic probes,[13−19] and the results are discussed in the relation to the local density enhancement, which is specific to the medium-density region of the SCFs.[20,21] Although these studies are useful, information about a specific site of the solute molecule is difficult to obtain by the spectroscopic measurements of the electronic states of the solute molecule.

Recently, our group has developed a new high-temperature and high-pressure optical system and succeeded in measuring resonance and nonresonance Raman spectra of solute molecules dissolved in SCW and SCMe.[22] For example, we measured the NO_2 stretching mode of *p*-nitroaniline in SCW[23] and found unique density dependence of the vibrational frequency shift. By using the same optical flow cell, we measured the Raman spectra of a reaction intermediate under supercritical condition, and the results are presented in this article.

The solvation of the reaction intermediate is an interesting issue in relation to the electronic structure of the solute molecule. Terazima has reported that several types of transient radicals in solution show slower diffusion than stable molecules with similar molecular sizes.[24] For example, the diffusion coefficient of the pyrazinyl radical produced by the hydrogen abstraction reaction in alcohols is about three times smaller than that of pyrazine in the same solvents. Similar slow diffusion of transient radicals has been reported in the solution of supercritical fluids.[25,26] For example, Ohmori et al. found that the diffusion of the benzophenone ketyl radical in SCMe was slower than the diffusion of benzophenone.[26] In addition, the relative value of the diffusion coefficient of the radical in comparison with the parent molecule was not strongly dependent on the solvent

* Corresponding author. Telephone: +81-75-753-4024. Fax: +81-75-753-4000. E-mail: ykimura@iic.kyoto-u.ac.jp.
[†] Graduate School of Science.
[‡] International Innovation Center.

10.1021/jp077245j CCC: $40.75
Published on Web 02/13/2008

density, which was varied from the ambient density to a density of about 1.5 times the critical density of the solvent.

According to ab initio calculations, the slow diffusion of the radical was explained by the large response of the electron distribution of the radical to the local electric field of the solvent molecule.[27] Supporting this theoretical prediction, Terazima and Hamaguchi found an interesting feature of Raman spectra of transient radicals.[28] They investigated the Raman spectra of the pyradinyl radical and the benzosemiquinone radical by time-resolved resonance Raman measurement and found that the Raman bandwidths of these radicals were larger than those of the corresponding parent molecules. For example, while the bandwidth of the C═O stretching mode of benzoquinone around 1664 cm^{-1} is 10 cm^{-1}, the bandwidth of C═O stretching mode of the semiquinone radical (1530 cm^{-1}) is 19 cm^{-1}. The large bandwidth suggests that the solvent fluctuation around the radical molecule is larger than the solvent fluctuation around the stable parent molecule. One of the aims of our study is to investigate the modification of this spectroscopic feature in supercritical fluids, in which the solvent fluctuation is enhanced.

Until now, the study of the reaction intermediate in SCFs by the time-resolved resonance Raman spectroscopy has been quite limited. To the best of our knowledge, Raman measurement of the triplet state of anthracene in supercritical carbon dioxide was the only case reported to date.[29] In this study, the resonance Raman spectrum of the triplet state of anthracene was probed at 416 nm after the excitation at 355 nm at two different temperatures of 35 and 55 °C and pressure ranging from 7 to 50 MPa. It was reported that the band assigned to the triplet state of anthracene did not show any changes with variations in temperature and pressure. However, this observation may be explained by the weak interaction between carbon dioxide and anthracene that is not capable of inducing the intramolecular structure change in anthracene.

In this article, we report a time-resolved resonance Raman study of the ketyl radical produced by the hydrogen abstraction reaction of decafluorobenzophenone (DFBP) in 2-propanol (Scheme 1). In relation with the previous work on the slow diffusion on benzophenone ketyl radical in supercritical alcohols,[26] the study on the vibrational spectra of ketyl radical under supercritical condition is the first to measure the Raman spectrum. We chose DFBP instead of benzophenone because the efficiency of the hydrogen abstraction by DFBP is much higher than that of benzophenone.[30] In addition, the ketyl radical of DFBP (DFBPK) is nonfluorescent, whereas the benzophenone ketyl radical is weakly fluorescent. These points are significant, since time-resolved resonance Raman measurements using high-pressure and high-temperature cells are difficult since the collection of the signal or the accessibility to the optical window is limited by the high-pressure equipment, and the efficiency of Raman scattering is important for obtaining high signal-to-noise (S/N) ratio. Anandhi and Umapathy have made detailed investigations of the Raman spectra of DFBP, the triplet state of DFBP, and DFBPK in solution.[31] They discussed the C═C stretching mode and the C═O (or C−O) stretching mode of these molecules in relation to their molecular structures. In the present study, we investigated the temperature dependence of the peak position and the bandwidth of the C═C and C−O stretching modes. To identify the differences in the solvent effect of the radical species and the stable molecule, we also measured the Raman spectra of stable molecules with molecular structures similar to that of DFBPK. We studied the C═C stretching modes of DFBP, decafluorobenzhydrol (DFBH), benzophenone (BP), and benzhydrol (BH), the C−O stretching mode of BH, and the C═O stretching modes of DFBP and BP (Scheme 1). The difference between the transient radical and stable molecules will be discussed.

SCHEME 1: Reaction Scheme of DFBP with 2-Propanol and Chemical Structures of Reference Samples

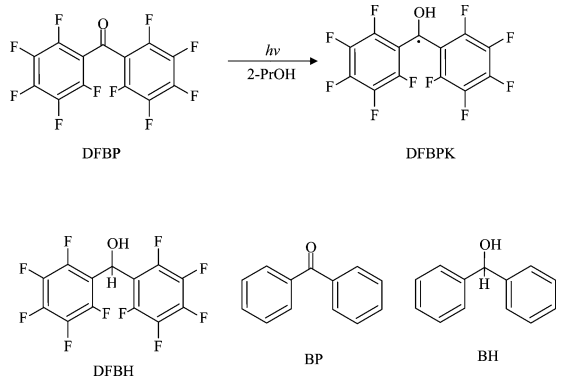

2. Experimental Section

2.1. Materials. DFBP (>98%) was purchased from Tokyo Kasei and was purified by recrystallization from ethanol before use. DFBH (>99%) and BH (>99%) were purchased from Tokyo Chemical Industry Co. and were purified by recrystallization from hexane. 2-Propanol (spectroscopic grade) and BP (guaranteed grade) were purchased from Nacalai Tesque and were used without further purification. Benzophenone-^{13}C (BP-^{13}C, carbonyl carbon ^{13}C > 99%) was purchased from CDS Isotopes and was used without further purification. Benzhydrol-^{13}C (BH-^{13}C, COH carbon is labeled by ^{13}C) was kindly supplied by Dr. Y. Matano (Kyoto University). It was synthesized by reduction of BP-^{13}C using $NaBH_4$ and was purified by column chromatography on silica gel. Organic solvents (cyclohexane (C_6H_{12})), carbon tetrachloride (CCl_4), chloroform ($CHCl_3$), acetonitrile (MeCN), tetrahydrofuran (THF), 2-propanol (2-PrOH), and methanol (MeOH): (spectroscopic grade) were purchased from Nacalai Tesque and were used as received. The critical temperature, pressure, and density of 2-propanol are 508.3 K, 4.76 MPa, and 273 kg m^{-3}, respectively.[32] The density of 2-propanol at different thermodynamic states was calculated by interpolating the values in the table in ref 33.

2.2. Time-Resolved Resonance Raman Measurement. To measure the time-resolved resonance Raman spectra in high-temperature and high-pressure fluids, we used a specially designed cell described elsewhere (see the schematic drawing in Supporting Information (SI) Figure S1).[22] A high-pressure cell was equipped with two sapphire windows (3.5-mm diameter, 2-mm thickness). The aperture angle of the window was 45° to collect the scattering from the sample effectively, and the optical path length was approximately 5 mm. The sample solution continuously flowed at 1.5 mL min^{-1} using an HPLC pump (JASCO; PU-2080plus or PU-1580). A freshly prepared sample solution was used for the measurement at each temperature and pressure, and the solution was being purged by dry nitrogen during the measurement. The pressure in the cell was controlled by a back pressure regulator (JASCO; 880-81) with an accuracy of about ±0.3 MPa. The temperature of the cell was regulated within the accuracy of ±1 K by a sheathed heater wounded around the cell and a thermocouple directly inserted in the sample chamber.

For the measurements of the time-resolved resonance Raman signal, the 355-nm third harmonic of a Nd:YAG laser (Con-

tinuum, Surelite II; ca. 5 ns, 10 Hz) was used as a pump pulse, and the 532-nm second harmonic of another Nd:YAG laser (Continuum, Minilite II; ca. 4 ns, 10 Hz) was used as a probe pulse. The two laser pulses were collinearly aligned and introduced into the sample cell. The spot size of the probe pulse on the sample solution was adjusted to about 0.5 mm in diameter by a convex lens (f (focal length) = 150 mm, D (diameter) = 60 mm). The spot size of the pump pulse was adjusted to be slightly larger than that of the probe pulse by a pair of convex and concave lenses. The Raman scattering was collected by a mirror (D = 100 mm) at the backscattering geometry and focused by a lens (f = 200 mm, D = 60 mm) on the entrance slit of a 23-cm monochromator (Acton, Spectra Pro 2300i, a 2400 lines mm^{-1} grating) equipped with an image intensifier integrated CCD camera (Princeton, PI-MAX102). The resolution of the CCD pixel was about 0.5 cm^{-1}. The Rayleigh scattering of the probe pulse was blocked by an edge filter (Semrock, RazorEdge LP02-532RS-25) placed in front of the entrance slit. The timing between the pump and probe pulses was tuned by the flash timing and Q-switch delay of both lasers triggered by a delay generator (Stanford, DG535). The detector gate width was set at 40 ns, and the exposure time was 5 s. The spectrum was accumulated for about 30 min. The concentration of DFBP was adjusted to approximately 20−30 mM. The Raman spectra were collected at the constant pressure of 31.2 MPa and at several temperatures (298, 350, 450, and 520 K).

The nonresonant Raman signal was detected using the 514.5-nm laser line of an Ar ion laser, and the system is described elsewhere.[34] The concentrations of BH and DFBH were adjusted to approximately 100 mM, and the concentrations of BP and DFBP were about 50 mM. The measurements were performed at constant pressure (30.0 MPa) at different temperatures (298, 350, 450, and 520 K). The measurements at 520 K and 10.0 MPa were also performed for all reference samples.

2.3. DFT Calculation. To make an assignment of the observed Raman band, the Raman spectrum of each molecule was calculated by the density functional theory (DFT) implemented in Gaussian 03.[35] We used the B3LYP model using the basis set of 6-31+G(d). For the calculation of the open shell molecule, the UB3LYP model was employed using the same basis set. All computations were carried out by Fujitsu Primepower HPC2500 in the Academic Center for Computing and Media Studies, Kyoto University.

3. Results

3.1. Time-Resolved Resonance Raman Spectra of DFBPK. According to ref 30, the hydrogen abstraction of DFBP by the photoexcitation in 2-propanol occurs fast, and DFBPK appears within 500 ns. We have also verified that the same reaction proceeds within 500 ns under conditions of high temperature and high pressure by the transient absorption measurement (SI, Figure S2).

Figure 1 shows the time-resolved resonance Raman spectra acquired at different delay times after the 355-nm excitation at 31.2 MPa and 298 K. The Raman bands that do not depend on the delay time are the solvent bands. The Raman bands that appear around 1274 and 1639 cm^{-1} after the photoexcitation are the bands attributed to DFBPK. By subtracting the solvent bands, we identified the Raman bands of DFBPK at different temperatures as shown in Figure 2a,b.

The band around 1639 cm^{-1} is assigned to the C═C stretching mode of phenyl rings that is closely related to the ph-8a (C═C stretching vibration of a phenyl ring) mode (1669 and 1648 cm^{-1} by the DFT calculation).[36] The peak position concurs with the reported value.[31] With increasing temperature, the band center shifts to a lower frequency and the bandwidth shows broadening. The S/N ratio at the elevated temperature is decreased. This may partially be the result of the optical windows becoming opaque due to condensation of the photochemical product. The peak position and the bandwidth at each experimental condition were evaluated by fitting the band to a Lorentzian function for 298 and 350 K and to a Gaussian function for 450 and 520 K. The results of the fits are shown by the dotted lines in Figure 2a.

The band around 1274 cm^{-1} is assigned to the C−O stretching mode of DFBPK, which includes some contribution from the ph-12 (radial skeletal vibration of a phenyl ring) mode (1282 cm^{-1} by the DFT calculation). The peak position concurs with the reported value.[31] As shown in Figure 2b, with increasing temperature the band shifts to a lower frequency,

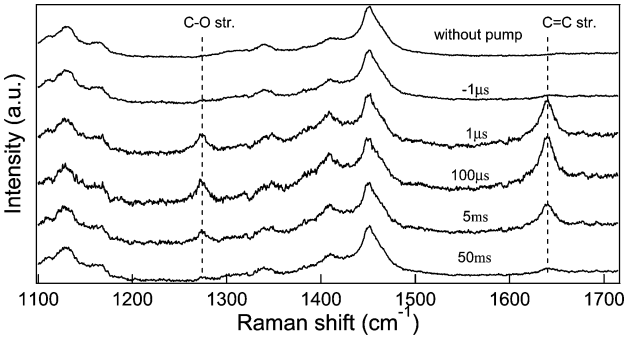

Figure 1. Time-resolved resonance Raman spectra of DFBP at several delay times after the photoexcitation at 355 nm probed by 532 nm at 298 K and 31.2 MPa.

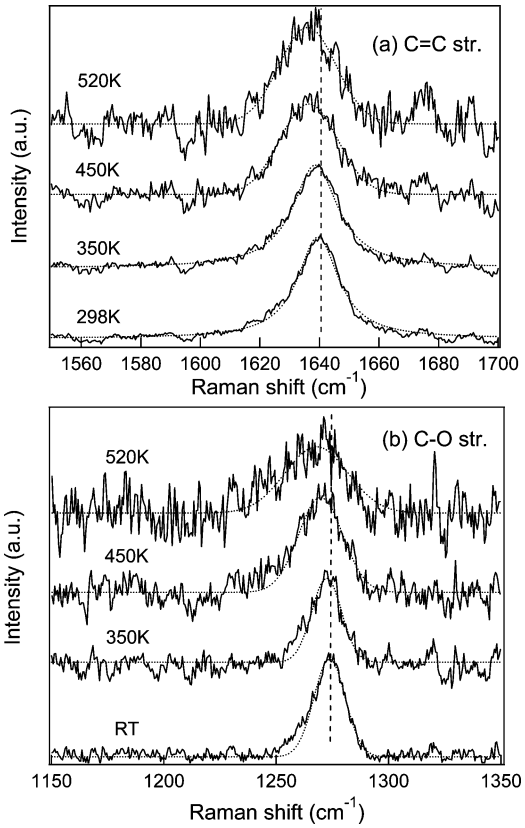

Figure 2. Temperature dependence of the time-resolved resonance Raman spectra of DFBPK at 31.2 MPa. The solid lines are the experimentally observed signals, and the broken lines are the best fits by the Lorentzian (or the Gaussian) function. (a) C═C stretching mode. (b) C−O stretching mode.

TABLE 1: Peak Frequency (ν_P) and Bandwidth ($\Delta\nu$; fwhm) of the C═C Stretching Mode and the C−O Stretching Mode of DFBPK at Different Temperatures[a]

T (K)	P (MPa)	ρ_r	ν_P(C═C)	$\Delta\nu$(C═C)	ν_P(C−O)	$\Delta\nu$(C−O)
298	31.2	2.95	1639.5	17	1273.8	16
458	31.2	2.81	1638.6	18	1273.3	17
350	31.2	2.44	1636.4	23	1269.8	23
520	31.2	2.13	1636.0	23	1268.3	

[a] The unit of frequency and bandwidth is cm^{-1}. ρ_r is the reduced density of the solvent scaled by the critical density of the solvent.

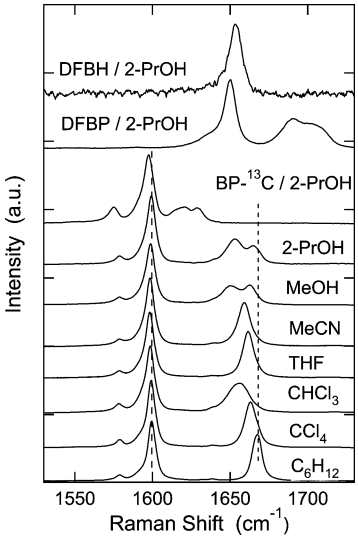

Figure 3. Raman spectra of DFBH, DFBP, and BP-^{13}C in 2-PrOH, and BP in various solvents.

while the band shape does not show significant temperature dependence. We estimated the peak position and the bandwidth of this mode by fitting the Raman band to a Gaussian function. Since the band shape is asymmetrical, we estimated the bandwidth by fitting mainly the higher frequencies of the spectrum as shown by the dotted lines in Figure 2b. The results are summarized in Table 1.

3.2. Raman Spectra of the Reference Materials. For reference molecules, we chose BH, BP, DFBP, and DFBH. However, we found that the C═C stretching mode and the C−O stretching mode of BH showed unexpected complexity and that BH cannot serve as a reference for the purpose of this experiment (see details in SI Figure S3). Therefore, we will present the results and analysis of the Raman spectra of the remaining reference molecules: BP, DFBP, and DFBH.

Figure 3 shows the Raman spectra of DFBH, DFBP, BP, and BP-^{13}C in 2-PrOH, as well as the spectra of BP in other solvents. The vibrational frequencies of the reference molecules in 2-PrOH are summarized in Table 2 together with the DFT calculation results. Although the C−O stretching mode of DFBH is expected to appear at 1084 cm^{-1} according to the DFT calculation, there was no corresponding band found between 950 and 1200 cm^{-1} in the spectrum. The bands at 1599 cm^{-1} in the Raman spectrum of BP, at 1650 cm^{-1} in the spectrum of DFBP, and at 1653 cm^{-1} in the spectrum of DFBH are assigned to the C═C stretching mode. This C═C stretching band of BP does not show any significant solvent effect. On the other hand, the stretching band in the spectrum of BP appearing in the high-frequency region, which could be assigned to the C═O stretching mode according to the DFT calculations, shows a significant solvent effect and even shows splitting in some solvents. Table 3 summarizes the results of BP in various solvents. The band around 1667 cm^{-1} in the spectrum of BP in C_6H_{12} shifts to a lower frequency with increasing solvent polarity and hydrogen-bonding ability. Only in the strongly hydrogen-bonding solvents, such as in MeOH and 2-PrOH, the band is split in two. Both split bands show isotope shifts of similar magnitude in 2-PrOH. Therefore, we consider that these bands represent differently solvated species of BP; the lower band represents strongly hydrogen-bonded BP and the higher band represents loosely solvated BP. In fact, there is a good linear correlation between the vibrational frequency of the C═O stretching mode and the solvent acceptor number (*AN*)[37] as shown in Figure 4. Several reports in the past have suggested that the vibrational frequency of the carbonyl stretch gives a good estimation of the *AN*.[38,39] For example, it was reported that the C═O stretching mode of diphenylcyclopropenone correlates well with *AN* of solvents.[39] In the present case, the correlation gives the following estimation (eq 1) of the solvent *AN* from the vibrational frequency of the C═O stretching mode of BP:

$$AN = 4035.9 - 2.422\nu\ (\mathrm{cm}^{-1}) \quad (R = -0.987) \qquad (1)$$

where ν is the frequency of the C═O mode (in the case of the splitting, the lower frequency band).

We turn to the temperature and density effects of each band in the Raman spectra of the reference samples. Figure 5 shows the Raman spectra of the reference compounds at different temperatures and pressure of 30 MPa, as well as the spectra of these molecules at 10 MPa and 520 K, and the Raman spectra of the solvent 2-PrOH. The Raman band assigned to the C═C stretching mode shifts to a lower frequency with increasing temperature. On the other hand, the C═O stretching modes of BP and DFBP shift to a higher frequency with increasing temperature. Particularly, the lower frequency band is significantly displaced with respect to the higher frequency band and causes a near overlap of the two bands at 520 K. To determine the peak position and bandwidth of each band at different temperatures, each Raman spectrum was fit to a sum of Lorentzian functions. Typical decompositions are shown for the

TABLE 2: Experimental and Calculated Vibrational Frequencies (cm^{-1}) of BP, BP-^{13}C, and DFBP

Raman[a]				DFT calculation[b]			assignment
DFBH	BP	BP-^{13}C	DFBP	DFBH	BP	DFBP	approximate description[c]
	1665	1629	1705		1718	1762	ν(C═O)
	1653	1621	1690				
1653	1599	1597	1650	1682	1650	1675.21	ν(C═C) (like the ν(ph-8a) vibration of each phenyl ring; in-phase and out-of-phase
				1677	1648	1675.15	motions of two rings)
1638				1659.9			ν(C═C) (like the ν(ph-8a) vibration of each phenyl ring; in-phase and out-of-phase
				1659.5			motions of two rings), γ(C−H)
				1084			ν(C−O), ν(ph-18)[d]

[a] Experimental data in 2-PrOH (off-resonance). [b] B3LYP/6-31G+(d). No scaling factor. [c] Nomenclature according to Varsanyi.[36] ν = stretching, γ = out-of plane deformation. [d] ph-18 = CH in-plane bending vibration.

TABLE 3: Experimental Vibrational Frequencies (cm^{-1}) of BP in Various Solvents and BP-^{13}C in 2-Propanol

solvents	ν(C═C)	ν(C═O)		AN[a]
C_6H_{12}	1600	1667		0
CCl_4	1599	1663		8.6
$CHCl_3$	1598	1655		23.1
THF	1598	1662		8
MeCN	1598	1659		18.9
MeOH	1599	1650	1663	41.5
2-PrOH	1599	1653	1665	33.5

[a] Reference 37.

Raman spectra of BP, DFBP, and DFBH at room temperature in Figure 5, and results of the fit are shown by the broken lines. The fitting appears successful, although some deviations are found in the tail regions of each band. In the case of 2-PrOH, the C−O stretching mode is observed at 953 cm^{-1} and two weaker bands assigned to the C−H bending motion are observed in the lower frequency region. At room temperature, these bands are simulated well by a sum of three Lorentzian functions. However, with increasing temperature, the overlapping of the three bands becomes significant, and two Lorentzian functions are sufficient to fit the data at temperatures above 450 K.

The peak positions and the bandwidths obtained by the spectrum fitting are summarized in Tables S1−S4 (SI). Figure 6a shows the change in the vibrational frequencies of the C═C stretching modes at different solvent densities relative to the frequency value at 30 MPa and 298 K. The horizontal scale in Figure 6a is the reduced density (ρ_r) scaled by the critical density of the solvent. In the cases of DFBH, BP, and DFBP, the strongest Raman bands at the higher frequency corresponding to the C═C stretching vibration are plotted (the band at 1653 cm^{-1} for DFBH, at 1599 cm^{-1} for BP, at 1650 cm^{-1} for DFBP at 298 K and 0.1 MPa). In all samples, the peak frequencies decrease with decreasing solvent density due to the increase in the temperature. The radical does not display any unique characteristics when compared with the reference molecules. It is noteworthy, however, that the fluorinated solutes (DFBP and DFBH) show larger shifts.

4. Discussion

We speculate that the main reason for the shift in the position of the C═C stretching bands to lower frequencies in all spectra is a decrease in the repulsive effect of the solvent with decreasing solvent density.[40−43] Figure 3, illustrating the solvent effect on both the C═C and the C═O stretching modes of BP, demonstrates that the vibrational frequency of the C═C stretching mode is hardly dependent on the solvent polarity and the hydrogen-bonding ability of the solvent. This means that the C═C stretching mode is insensitive to the attractive interaction between molecules, possibly due to the distribution of this stretching mode over the aromatic rings of the molecule. By decreasing the solvent density from 2.9 to 2.0, the solvent packing effect is drastically reduced, which results in the reduction of the repulsive effect. Generally, repulsive interaction between solute and solvent increases the vibrational frequency, and therefore reduction in the repulsive effect due to lower solvent density would be expected to decrease the frequency of the bands as we observed.[40]

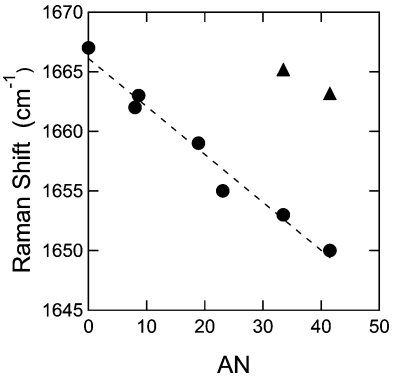

Figure 4. Correlation between *AN* of various solvents and the vibrational frequency of the C═O stretching mode of BP. The triangles represent the peak frequency of the higher frequency band in case of splitting.

In support of our conclusions, it has been previously reported that the breathing (ph-1) mode of the phenyl ring of hexafluorobenzene (HFB) in HFB (557 cm^{-1}) monotonically increases with solvent density by about 2 cm^{-1} from $\rho_r = 2.0$ to 3.0.[43] In the medium-density region below $\rho_r = 2.0$, the peak shift becomes small along the isotherm near the critical temperature. The authors used a hard diatomic model in a hard sphere solvent developed by Ben-Amotz et al.[41,42] and calculated the density dependence of the vibrational frequency. They demonstrated that a vibrational frequency shift at the higher density is due to the repulsive interaction between molecules and that a smaller density effect near the critical point was due to the effect of the attractive interaction and the local density enhancement. We consider that a similar effect of the repulsive interaction is observed in the frequency shift in our study at the higher density region, although we could not survey the density region near the critical point where the attractive interaction is more dominant. However, the application of the hard diatomic model used in the theoretical calculation is difficult in our study, since the C═C stretching mode spread over two phenyl rings.

Figure 6b shows the reduced density dependence of the C−O and C═O stretching frequencies. In the cases of BP and DFBP, the peak positions of the lower frequency bands that show a significant solvent effect are plotted. The vibrational frequency of the C−O stretching mode of DFBPK decreases with decreasing solvent density, and the solvent density dependence is similar to the case of the C−O stretching mode of 2-PrOH. The extent of the frequency shift of the C−O stretch of DFBPK is quite large (∼5 cm^{-1}) and is comparable to the frequency shift of the C−O stretch of 2-PrOH. This similarity indicates that the structure of DFBPK is affected by a change in the environment around the C−OH group to a similar extent as 2-PrOH is affected. On the other hand, the peak frequency of the C═O band of DFBP and BP increases with decreasing density. As mentioned in section 3.2 (Figure 4), the peak position of the lower-frequency band of the C═O stretching mode of BP is an indicator of the solvent Lewis acidity (*AN*). By using eq 1, the values of *AN* of 2-PrOH at high temperatures can be estimated; *AN* varies from 36 at 298 K to 9.5 at 520 K and 10 MPa (Table S3 in SI). A remarkable decrease in the hydrogen-bonding ability of water and alcohols with temperature increasing up to the supercritical temperature has already been demonstrated by NMR measurements,[7,8] and our result is consistent with these previous studies. The decrease in the vibrational frequency of the C−O stretching modes of DFBPK and 2-PrOH with decreasing solvent density can be explained by the decrease of the Lewis acidity of the solvent. The decrease of the *AN* indicates that the strength of the hydrogen bonding of the solute acting as a proton acceptor with the solvent as the proton donor becomes weak with a decrease of the solvent density. Similarly, the hydrogen bonding of the solute, which acts as a proton donor, is expected to decrease. As a result of

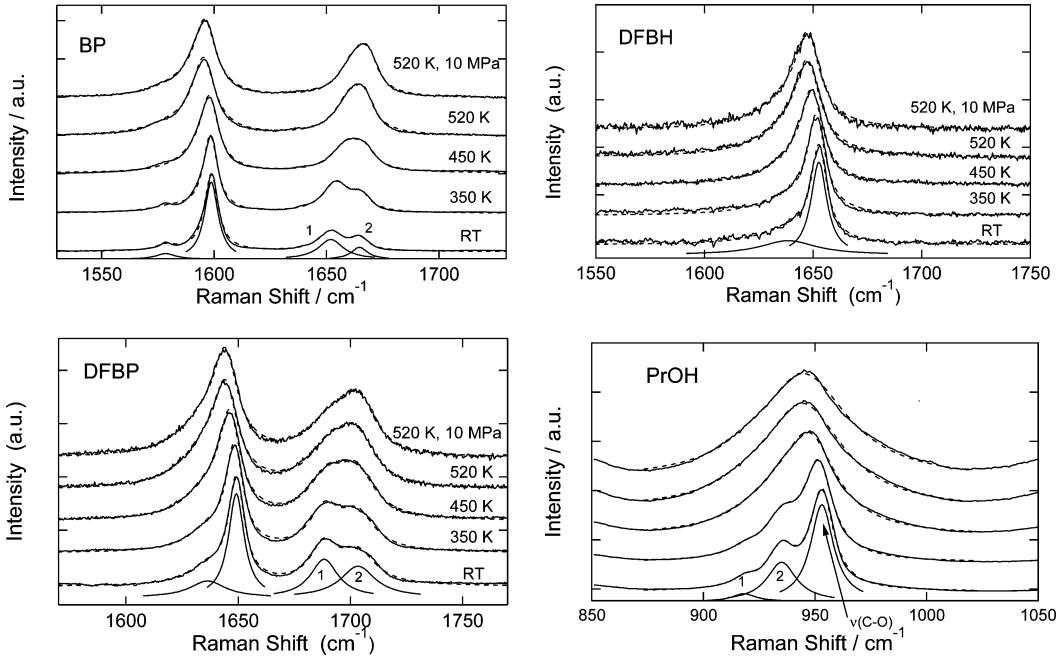

Figure 5. Raman spectra of BP, DFBP, and DFBH around the C═C and C═O stretching frequency region at various temperatures and 30.0 MPa, together with the spectra of 2-PrOH around the C−O stretching region. The spectra at 520 K and 10.0 MPa are also included. The solid lines are experimental results. The Lorentzian functions shown below the signal at 298 K represent the spectral decomposition of the signal at 298 K as a typical example. The broken lines are the simulated signals by a sum of Lorentzian functions.

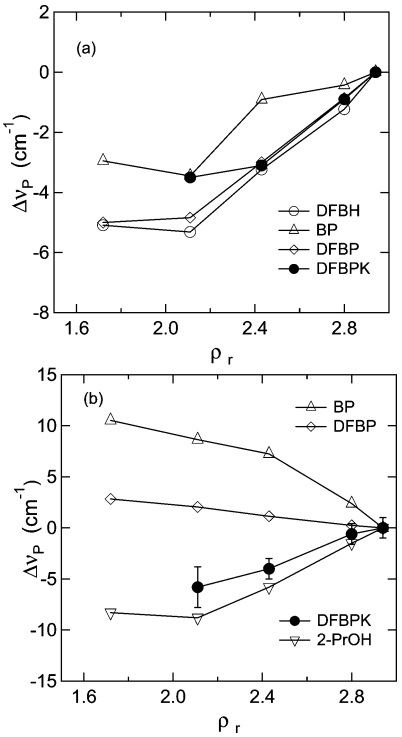

Figure 6. Peak shifts for (a) the C═C stretching modes and (b) the C═O or C−O stretching mode relative to the value at 30.0 MPa and 298 K, respectively. For simplicity, only one vibrational mode is plotted in the case of split bands. For the C═C stretching mode of other molecules, the main large modes are plotted; for the C═O stretching modes of BP and DFBP, the lower frequency bands (band 1, Figure 5) are plotted.

these effects, an increase of the OH bond strength occurs, which results in the concomitant decrease in the C−O bond strength. Preliminary DFT calculations of the 1:1 hydrogen-bonded cluster of BH and alcohol molecules also predict a shift to a higher frequency of the C−O band by forming a complex with the solvent,[44] although the complexity due to the splitting of the C−O band of BH makes it difficult to compare with other cases in this experiment (SI Figure S3).

It is important to note the difference in the bandwidth between DFBPK and the reference samples. Even if we consider the effect of the slit function for the different experimental systems used for the measurement,[45] the bandwidth of the C═C stretching mode of DFBPK (17 cm^{-1} at 298 K, Table 1) is about 1.5 times larger than the bandwidths of the reference samples (e.g., 10 cm^{-1} for DFBH; Table S1 and Figure S4). Therefore, the previous finding that the Raman bandwidth of the intermediate radical is larger than that of the stable molecule is confirmed in the present study.[28] Considering that the C═C stretching mode is related to the deformation of the phenyl ring, the wider bandwidth of the radical indicates the relative fragility of the phenyl ring of the radical to the applied external force field. On the other hand, the bandwidth of the C−O stretching mode of DFBPK is close to that of the C═O stretching mode of BP (SI). This is probably due to the fluctuations in the hydrogen bonding affecting both the C═O stretching mode and the C−O stretching mode and causing band broadening (16 cm^{-1} for DFBPK and 15 cm^{-1} for DFBP). The frequency of the C−O stretching mode of DFBPK is sensitive to the environment around the C−O−H group. Therefore, the large bandwidth of the C−O stretching mode of DFBPK is explained by the fluctuation in the bond strength due to the movement of surrounding solvent molecules. Large fluctuation, or deformability, of the C−O bond and the phenyl ring of DFBPK due to solvent and thermal fluctuations may be related to the slower diffusion of the reaction intermediate radicals at various temperatures and pressures.[24−26] The structural deformability enhances the polarizability of the radical due to the external field and strengthens the solute−solvent interaction.[27]

5. Conclusions

In the present study, we investigated the Raman spectra of the transient radical DFBPK and related compounds at high temperatures and high pressures in 2-propanol. It has been found

that the vibrational frequencies of the C═C stretching modes decreased with increasing temperature, reflecting the decrease in the repulsive effect due to the decrease of the packing fraction. On the other hand, the C−O stretching mode of DFBPK and the C═O stretching mode of BP and DFBP were sensitive to the change of the attractive interaction between solvent and the solute. We have also found that the vibrational frequency of the C═O stretching mode of BP is a good indicator of the solvent *AN*. The value of the *AN* of 2-propanol changes from 36 at 298 K to 9.5 at 520 K and 10 MPa. In agreement with the change in *AN*, the vibrational frequency of the C−O stretching mode of DFBPK decreases. The vibrational bandwidths of DFBPK were generally large, which indicated the deformability of the radical. Particularly, the bandwidth of the C═C stretching mode of the radical was more than 1.5 times larger than the corresponding modes of stable molecules under various conditions. The bandwidth of the C−O stretching mode of the radical was similar to the C═O stretching mode of BP. The deformability and the sensitivity of the structure of DFBPK to solvent fluctuations may be related to the slower diffusion of the reaction intermediate radicals.

In the present study, we were not able to measure the time-resolved resonance Raman spectra for the density region below $\rho_r = 2$ where unique solvation, such as local density enhancement, has been observed thus far. Since we could detect the transient absorption of DFBPK for the lower density region at 520 K (not presented here), it may be possible to measure the Raman signal by improving the S/N in the future. The development of the system is now under way to survey the density dependence of the radical Raman at the supercritical temperature, and we hope to relate our study to the local density effect on the Raman peak shift of the radical in the near future.

Acknowledgment. We are very grateful to Dr. Yoshihiro Matano and Mr. Tooru Miyajima (Kyoto University) for the preparation of BH-^{13}C from BP-^{13}C. This work is partially supported by Grants-in-Aid for Scientific Research from JSPS (Nos. 16350010 and 19350010) and by the fund from the Mitsubishi Foundation.

Supporting Information Available: Tables of the results of fits to the sum of Lorentzian functions for the C═C and the C−O or the C═O stretching modes of DFBH, BP, DFBP, and 2-PrOH. Figures for the experimental setups, the transient absorption spectra of DFBPK under high temperature and high pressure, the Raman spectra of BH and BH-^{13}C, and the solvent density dependence of the Raman bandwidths. This material is available free of charge via the Internet at http://pubs.acs.org.

References and Notes

(1) Weingärtner, H.; Franck, E. U. *Angew. Chem., Int. Ed.* **2005**, *44*, 2672.

(2) Bermejo, M. D.; Cocero, M. J. *AIChE J.* **2006**, *52*, 3933.

(3) de Castro, R. E. N.; Vidotti, G. J.; Rubira, A. F.; Muniz, E. C. *J. Appl. Polym. Sci.* **2006**, *101*, 2009.

(4) Kamitanaka, T.; Matsuda, T.; Harada, T. *Tetrahedron* **2007**, *63*, 1429.

(5) Psotrino, P.; Tromp, R. H.; Ricci, M. A.; Soper, A. K.; Neilson, G. W. *Nature* **1993**, *366*, 688.

(6) Yamaguchi, T.; Yoshida, K.; Yamamoto, N.; Hosokawa, S.; Inui, M.; Baron, A. Q. R.; Tsutsui, S. *J. Phys. Chem. Solids* **2005**, *66*, 2246.

(7) (a) Matubayasi, N.; Wakai, C.; Nakahara, M. *J. Chem. Phys.* **1997**, *107*, 9133; **1999**, *110*, 8000. (b) Matubayasi, N.; Nakao, N.; Nakahara, M. *J. Chem. Phys.* **2001**, *114*, 4107.

(8) Hoffmann, M. M.; Conradi, M. S. *J. Phys. Chem. B* **1998**, *102*, 263.

(9) (a) Asahi, N.; Nakamura, Y. *Chem. Phys. Lett.* **1998**, *290*, 63. (b) Asahi, N.; Nakamura, Y. *J. Chem. Phys.* **1998**, *109*, 9879.

(10) Ikushima, Y.; Hatakeda, K.; Saito, N.; Arai, K. *J. Chem. Phys.* **1998**, *108*, 5855.

(11) (a) Tassaing, T.; Danten, Y.; Besnard, M. *J. Mol. Liq.* **2002**, *101*, 149. (b) Lalanne, P.; Andanson, J. M.; Soetens, J. C.; Tassaing, T.; Danten, Y.; Besnard, M. *J. Phys. Chem. A* **2004**, *108*, 3902.

(12) Saitow, K.; Sasaki, J. *J. Chem. Phys.* **2005**, *122*, 104502.

(13) Bennett, G. E.; Johnston, K. P. *J. Phys. Chem.* **1994**, *98*, 441.

(14) Niemeyer, E. D.; Dunbar, R. A.; Bright, F. V. *Appl. Chem.* **1997**, *51*, 1547.

(15) Osada, M.; Toyoshima, K.; Mizutani, T.; Minami, K.; Watanabe, M.; Adschiri, T.; Arai, K. *J. Chem. Phys.* **2003**, *118*, 4573.

(16) Kometani, N.; Takemiya, K.; Yonezawa, Y.; Amita, F.; Kajimoto, O. *Chem. Phys. Lett.* **2004**, *394*, 85.

(17) Oka, H.; Kajimoto, O. *Phys. Chem. Chem. Phys.* **2003**, *5*, 2535.

(18) Minami, K.; Mizuta, M.; Suzuki, M.; Aizawa, T.; Arai, K. *Phys. Chem. Chem. Phys.* **2006**, *8*, 2257.

(19) Blugarevich, D. S.; Sako, T.; Sugeta, T.; Ohtake, K.; Takebayashi, Y.; Kamizawa, C. *J. Chem. Phys.* **1999**, *111*, 4239.

(20) Kajimoto, O. *Chem. Rev.***1999**, *99*, 355.

(21) Tucker, S. C. *Chem. Rev.* **1999**, *99*, 391.

(22) (a) Fujisawa, T.; Maru, E.; Amita, F.; Harada, M.; Uruga, T.; Kimura, Y. In *Water, Steam, and Aqueous Solutions for Electric Power: Advances in Science and Technology*, Proceedings of the 14th International Conference on the Properties of Water and Steam, Kyoto, Japan, Aug 29−Sept 3, 2004; p 445. (b) Kimura, Y.; Amita, F.; Fujisawa, T. *Rev. High Pressure Sci. Technol.* **2006**, *16*, 87.

(23) Fujisawa, T.; Terazima, M.; Kimura, Y.; Maroncelli, M. *Chem. Phys. Lett.* **2006**, *430*, 303.

(24) Terazima, M. *Acc. Chem. Res.* **2000**, *33*, 687 and references therein.

(25) Kimura, Y.; Kanda, D.; Terazima, M.; Hirota, N. *J. Phys. Chem. B* **1997**, *101*, 4442.

(26) Ohmori, T.; Kimura, Y.; Hirota, N.; Terazima, M. *J. Phys. Chem. B* **2003**, *107*, 5958.

(27) (a) Morita, A.; Kato, S. *J. Am. Chem. Soc.* **1997**, *119*, 4021. (b) Morita, A.; Kato, S. *J. Chem. Phys.* **1998**, *108*, 6809.

(28) Terazima, M.; Hamaguchi, H. *J. Phys. Chem.* **1995**, *99*, 7891.

(29) Hegarty, J. N. M.; McGarvey, J. J.; Bell, S. E. J.; Al-Obaidi, A. H. R. *J. Phys. Chem.* **1996**, *100*, 15704.

(30) Shoute, L. C. T.; Mittal, J. P. *J. Phys. Chem.* **1993**, *97*, 8630.

(31) Anandhi, R.; Umapathy, S. *J. Raman Spectrosc.* **2000**, *31*, 331.

(32) Reid, R. C.; Prausnitz, J. M.; Poling, B. E. *The Properties of Gases and Liquids*, 4th ed.; McGraw-Hill: New York, 1987.

(33) Golubev, I. F.; Vasil'kovskyaya, T. N. *Inzh.-Fiz. Zh.* **1980**, *38*, 668.

(34) Fujisawa, T.; Terazima, M.; Kimura, Y. *J. Chem. Phys.* **2006**, *124*, 184503.

(35) Frisch, M. J.; Trucks, G. W.; Schlegel, H. B.; Scuseria, G. E.; Robb, M. A.; Cheeseman, J. R.; Montgomery, J. A., Jr.; Vreven, T.; Kudin, K. N.; Burant, J. C.; Millam, J. M.; Iyengar, S. S.; Tomasi, J.; Barone, V.; Mennucci, B.; Cossi, M.; Scalmani, G.; Rega, N.; Petersson, G. A.; Nakatsuji, H.; Hada, M.; Ehara, M.; Toyota, K.; Fukuda, R.; Hasegawa, J.; Ishida, M.; Nakajima, T.; Honda, Y.; Kitao, O.; Nakai, H.; Klene, M.; Li, X.; Knox, J. E.; Hratchian, H. P.; Cross, J. B.; Bakken, V.; Adamo, C.; Jaramillo, J.; Gomperts, R.; Stratmann, R. E.; Yazyev, O.; Austin, A. J.; Cammi, R.; Pomelli, C.; Ochterski, J. W.; Ayala, P. Y.; Morokuma, K.; Voth, G. A.; Salvador, P.; Dannenberg, J. J.; Zakrzewski, V. G.; Dapprich, S.; Daniels, A. D.; Strain, M. C.; Farkas, O.; Malick, D. K.; Rabuck, A. D.; Raghavachari, K.; Foresman, J. B.; Ortiz, J. V.; Cui, Q.; Baboul, A. G.; Clifford, S.; Cioslowski, J.; Stefanov, B. B.; Liu, G.; Liashenko, A.; Piskorz, P.; Komaromi, I.; Martin, R. L.; Fox, D. J.; Keith, T.; Al-Laham, M. A.; Peng, C. Y.; Nanayakkara, A.; Challacombe, M.; Gill, P. M. W.; Johnson, B.; Chen, W.; Wong, M. W.; Gonzalez, C.; Pople, J. A. *Gaussian 03;* Gaussian, Inc.: Wallingford, CT, 2004.

(36) Varsanyi, G. *Vibrational Spectra of Benzene Derivatives;* Academic Press: New York, 1969.

(37) See, for example: Reichardt, C. *Solvents and Solvent Effects in Organic Chemistry;* VCH: Weinheim, Germany, 1988.

(38) (a) Liu, Q.; Xu, X.; Sang, W. *Spectrochim. Acta, Part A* **2003**, *59*, 471. (b) Liu, Q.; Fang, D.; Zheng, J. *Spectrochim. Acta, Part A* **2004**, *60*, 1453.

(39) (a) Kimura, Y.; Fukuda, M.; Fujisawa, T.; Terazima, M. *Chem. Lett.* **2005**, *34*, 338. (b) Fujisawa, T.; Fukuda, M.; Terazima, M.; Kimura, Y. *J. Phys. Chem. A* **2006**, *110*, 6164.

(40) Schweizer, K. S.; Chandler, D. *J. Chem. Phys.* **1982**, *76*, 2296.

(41) Ben-Amotz, D.; Lee, M.-R.; Cho, S. Y.; List, D. J. *J. Chem. Phys.* **1992**, *96*, 8781.

(42) Ben-Amotz, D.; Herschbach, D. R. *J. Phys. Chem.* **1993**, *97*, 2295.

(43) Cabaço, M. I.; Besnard, M.; Tassing, T.; Danten, Y. *J. Mol. Liq.* **2006**, *125*, 100.

(44) We have calculated the 1:1 complex between BH and methanol, where the hydrogen atom of BH is solvated by OH of methanol. According to the optimized structure using the basis set of 6-31+G(d), the vibrational mode at 1059 cm^{-1} for bare BH is shifted to 1070 cm^{-1}, and the mode at

1045 cm^{-1} is shifted to 1051 cm^{-1}. The latter band of the complex does not have the contribution of C−O stretching in contrast to that of the bare BH molecule.

(45) A wider slit width was used to collect time-resolved resonance Raman spectra to increase the signal intensity. Therefore, the apparent bandwidth of the signal is broadened by the effect of the slit function; for example, the Raman signal at 1347 cm^{-1} of cyclohexane has the bandwidth of 18.6 cm^{-1} for the time-resolved system, while it has the bandwidth of 17.2 cm^{-1} for the static measurement system. For other bands, the bandwidths measured by the time-resolved system are generally at most 2 cm^{-1} larger than the bandwidths of the system for the static measurement. Therefore, the effect of the difference of the slit function is small and does not exceed 2 cm^{-1} for the results presented here.